Received: 29 November 2023 | Revised: 12 February 2024 | Accepted: 12 February 2024

DOI: 10.1002/ar.25415

RESEARCH ARTICLE

The Anatomical Record WILEY

The impact of measurement technique and sampling on estimates of skeletal muscle fibre architecture

Andrea B. Taylor[1] | **Claire E. Terhune**[2] | **Callum F. Ross**[3] | **Christopher J. Vinyard**[4]

[1]Department of Foundational Biomedical Sciences, Touro University California, Vallejo, California, USA

[2]Department of Anthropology, University of Arkansas, Fayetteville, Arkansas, USA

[3]Department of Organismal Biology and Anatomy, The University of Chicago, Chicago, Illinois, USA

[4]Biomedical Sciences, Ohio University—Heritage College of Osteopathic, Medicine, Athens, Ohio, USA

Correspondence
Andrea B. Taylor, Department of Foundational Biomedical Sciences, Touro University California, Vallejo, CA 94459, USA.
Email: ataylor11@touro.edu

Christopher J. Vinyard, Biomedical Sciences, Ohio University—Heritage College of Osteopathic, Medicine, Athens, OH 45701, USA.
Email: vinyard@ohio.edu

Funding information
National Science Foundation, Grant/Award Numbers: BCS 0452160, 0962677

Abstract

Skeletal muscle fibre architecture provides important insights into performance of vertebrate locomotor and feeding behaviours. Chemical digestion and in situ sectioning of muscle bellies along their lengths to expose fibres, fibre orientation and intramuscular tendon, are two classical methods for estimating architectural variables such as fibre length (L_f) and physiological cross-sectional area (PCSA). It has recently been proposed that L_f estimates are systematically shorter and hence less accurate using in situ sectioning. Here we addressed this hypothesis by comparing L_f estimates between the two methods for the superficial masseter and temporalis muscles in a sample of strepsirrhine and platyrrhine primates. Means or single-specimen L_f estimates using chemical digestion were greater in 17/32 comparisons (53.13%), indicating the probability of achieving longer fibres using chemical digestion is no greater than chance in these taxonomic samples. We further explored the impact of sampling on scaling of L_f and PCSA in platyrrhines applying a bootstrapping approach. We found that sampling—both numbers of individuals within species and representation of species across the clade significantly influence scaling results of L_f and PCSA in platyrrhines. We show that intraspecific and clade sampling strategies can account for differences between previously published platyrrhine scaling studies. We suggest that differences in these two methodological approaches to assessing muscle architecture are relatively less consequential when estimating L_f and PCSA for comparative studies, whereas achieving more reliable estimates within species through larger samples and representation of the full clade space are important considerations in comparative studies of fibre architecture and scaling.

KEYWORDS
chemical dissection, masseter, muscle dissection, PCSA, temporalis

1 | INTRODUCTION

It is well appreciated that skeletal muscles are the motors that drive many of the movements and forces associated with a range of behaviours. Comparative studies of vertebrate myology correlate with a variety of functional and evolutionary components of locomotor (Abdala et al., 2008; Anapol & Barry, 1996; Fleagle, 1977; Payne et al., 2006; Roberts & Scales, 2002; Stanchak & Santana, 2018), positional (Organ et al., 2009) and feeding behaviours (Curtis & Santana, 2018; Herrel & O'Reilly, 2006; Penrose et al., 2020; Pfaller et al., 2011; Santana et al., 2010;

Scales et al., 2016). Muscle fibre architecture—the length and internal arrangement of fibres relative to the force-generating axis of the muscle—is an important determinant of whole muscle function (Gans, 1982; Lieber, 2010). More specifically, fibre length (L_f) is proportional to whole-muscle excursion (and, by extension, velocity of contraction; Close, 1972; Bodine et al., 1982) and muscle force is proportional to muscle physiological cross-sectional area (PCSA) (Powell et al., 1984). Thus, studies of fibre architecture provide valuable insights into how variation in muscle morphology contributes to function and performance both within and among species.

Early studies of muscle anatomy were focused on descriptions of muscle presence/absence, size, position on the skeleton, groups and subdivisions based on fascial planes, development and innervation patterns (e.g., Allen, 1880; Bardeen, 1906; Bijvoet, 1908; Gregory & Camp, 1918; Howell, 1926). These kinds of studies continued into the second half of the 20th century (e.g., Turnbull, 1970) but by then, researchers were also using chemical digestion to dissolve the surrounding connective tissue, thereby facilitating the separation of muscle fibre bundles for microscopic visualization and estimation of fibre lengths and number of sarcomeres in series (Gans, 1982; Sacks & Roy, 1982; Williams & Goldspink, 1971). Following the pioneering work of Gans (1982) and Gans and Bock (1965), researchers were quantifying muscle architecture using chemical fixation of muscles in situ followed by dissection *en masse* of whole muscles from their skeletal attachments. Whole muscle mass, fibre length estimated from chemically digested fibre bundles, pinnation (typically approximated from surface measurements in one dimension) and an estimate of the specific density of muscle were used to compute PCSA (e.g., Sacks & Roy, 1982), using the following equation: $\text{PCSA} = [(\text{mass} \times \cos\theta)/(\text{fibre length} \times \text{specific density of muscle})]$, where θ is angle of pinnation.

In a departure from the use of chemical digestion, Anapol and Jungers (1986) sectioned fixed muscles along their belly lengths and incorporated in situ measures of fibre length by sampling fibres between their proximal and distal tendon attachments, rather than as isolated bundles. Because fibres between attachment sites may comprise shorter, overlapping segments rather than one long continuous segment (Huxley, 1957), the rationale for this approach is that it captures the full length of fibres as they contract and generate tension, either between intramuscular tendon attachments or between tendon attachment and bone (Anapol, 1984). These authors further estimated pinnation angle for each measured fibre bundle (=fasciculus) by multiplying fibre length by the cosine of the angle between fibre length and its tendon attachments, and calculated PCSA using the same equation noted above. Following Haxton (1944), they used the term 'reduced physiological cross-sectional area' (RPCA) to indicate that RPCA 'combines muscle mass with the length and angle of pinnation of the constituent fibres to derive a representative estimate of the maximum force deliverable by a quantity of muscle' (Anapol et al., 2008, p. 202). To account for joint posture-dependent variation in fibre length at the time of fixation, Anapol and Barry (1996) refined their measurement protocol to normalize fibre lengths measured in situ by an estimate of resting sarcomere length and used sarcomere-adjusted fibre length in their calculations of RPCA (see also Felder et al., 2005; Taylor et al., 2019).

Imaging techniques such as diffusible iodine-based contrast enhanced computed tomography (diceCT) (Jeffery et al., 2011; Metscher, 2009; Santana, 2018) have since gained popularity as less destructive methods to chemical digestion or muscle sectioning after fixation. Currently, however, imaging methods cannot resolve the microstructure of the muscle fibre to enable sarcomere length measurements. Some amount of muscle destruction remains necessary to estimate sarcomere lengths in vitro, which is essential both to normalize fibre lengths for joint-dependent variation associated with joint angle at fixation, and for ex vivo dynamic force calculations. Thus, both chemical digestion (e.g., Curtis & Santana, 2018) and muscle sectioning (e.g., Butcher et al., 2019; Myatt et al., 2011; Young et al., 2022) continue to be routinely employed for estimating fibre architecture measures.

Recently, the accuracy of in situ fibre length measurements sampled by sectioning muscle bellies along probable lines of action has been questioned. Specifically, it has been proposed that sectioning muscles along their bellies results in shorter fascicle measurements compared to chemical digestion (Hartstone-Rose et al., 2018). Although researchers have been using both chemical digestion and in situ muscle sectioning for decades, no studies have compared results obtained using these two methods. We address this gap in understanding through the following two aims. First, we retrospectively compare architecture results obtained from chemical digestion to those obtained by in situ muscle sectioning in a sample of strepsirrhine and platyrrhine primates. We use these data to test the hypothesis proposed by Hartstone-Rose et al. (2018) that employing chemical digestion results in consistently longer fibres than fibre length estimates obtained from sectioning muscle bellies.

Hartstone-Rose et al. (2018) also argued that methodological differences between their study and that of Taylor et al. (2015) account for the discordance of scaling relationships for architectural measures of chewing muscles in platyrrhines. Specifically, in their study of scaling relationships of the masseter and temporalis muscles in

TABLE 1 Sample sizes and source of material used in this study.

	This study[a]		Perry et al. (2011)[b]	
	n **(M, F, unknown)**	**Source**	***n*** **(M, F, unknown)**	**Source**
Cheirogaleus medius	3 (3, 0, 0)	DLC, MCZ	1 (1, 0, 0)	DLC
Eulemur coronatus	2 (2, 0, 0)	DLC	1 (1, 0, 0)	DLC
Eulemur macaco	1 (1, 0, 0)	DLC	1 (0, 1, 0)	DLC
Eulemur mongoz	3 (3, 0, 0)	DLC	1 (0, 1, 0)	DLC
Galago senegalensis	1 (1, 0, 0)	NMNH	2 (0, 2, 0)	ASU
Hapalemur griseus	6 (4, 2, 0)	DLC, PBZT	2 (0, 2, 0)	DLC
Lemur catta	5 (1, 1, 3)	MCZ, NCZ, PBZT	1 (0, 1, 0)	Duke
Mirza coquereli	1 (0, 1, 0)	DLC	1 (0, 1, 0)	DLC
Nycticebus coucang	3 (2, 0, 1)	DLC, CMNH, MCZ	1 (1, 0, 0)	Duke
Nycticebus pygmaeus	1 (1, 0, 0)	DLC	1 (0, 1, 0)	DLC
Otolemur garnetti	4 (0, 0, 4)	DLC, VU	2 (2, 0, 0)	ASU, Haines
Propithecus coquereli	3 (3, 0, 0)	DLC	3 (1, 2, 0)	DLC
Propithecus tattersalli	3 (1, 2, 0)	DLC	1 (1, 0, 0)	DLC
Varecia rubra	3 (1, 2, 0)	DLC	2 (1, 0, 1)	AMNH, DLC
	This study		**Hartstone-Rose et al. (unpub. data)**	
Callithrix jacchus	19 (7, 10, 2)	WRPRC	1 (1, 0, 0)	US
Saguinus oedipus	11 (2, 6, 3)	NERPRC	1 (0, 1, 0)	Zoos in Spain
Saimiri sciureus	15 (3, 10, 2)	SMBRR, NERPRC	2 (1, 1, 0)	Zoos in Spain
Sapajus apella	18 (7, 11, 0)	AM, NMNH, UC	3 (0, 2, 1)	Zoos in Spain

[a]DLC, Duke Lemur Center, NC; MCZ, Museum of Comparative Zoology, Cambridge (MA); NMNH, National Museum of Natural History, Washington, DC; PBZT, Parc Botanique et Zoologique de Tsimbazaza, Madagascar; NCZ, North Carolina Zoo; CMNH, Cleveland Museum of Natural History, Cleveland; VU, Vanderbilt University; WRPRC, Wisconsin National Primate Research Center, Madison; NERPRC, Emory National Primate Research Center, Atlanta; SMBRR, Squirrel Monkey Breeding and Research Resource; AM, Museum of Anthropology, Zurich; UC, University of Chicago, Chicago.
[b]Sources of material as reported in Perry et al. (2011) and Hartstone-Rose et al. (2018).

platyrrhines, Taylor et al. (2015) found that fibre lengths and PCSAs scale with significant negative allometry relative to load-arm estimates for incision and chewing across a sample of 15 genera representing 21 platyrrhine species ($n = 116$ individuals). Hartstone-Rose et al. (2018) were unable to replicate these findings in their subsequent analysis of seven platyrrhine genera representing 10 platyrrhines species ($n = 14$ individuals). They attributed discrepancies between the two studies to differences in methods used to estimate fibre length. However, these two studies also differ markedly in sampling—a two-fold difference in genera and species and more than eight-fold difference in number of individuals. Given these competing (but not mutually exclusive) considerations, we ask whether differences in sampling could account for the differences in findings between these two studies. Our second aim thus explores the impact of sampling on scaling estimates of muscle fibre length and PCSA in platyrrhines. In doing so, we consider the relative significance of these two factors—methods of collecting architectural data and sampling—on our understanding of masseter and temporalis muscle architecture across platyrrhines.

2 | MATERIALS AND METHODS

2.1 | Samples

To address the hypothesis that fibre length estimates are systematically longer after chemical digestion versus in situ muscle sectioning, we used previously collected data on in situ fibre length measurements after sectioning of the masseter and temporalis muscles for 14 strepsirrhine ($n = 39$ individuals) and four platyrrhine ($n = 63$ individuals) species (Table 1). The data used to address this hypothesis were previously collected by the first author as part of a larger project on primate fibre architecture. Some of the fibre length data for the four platyrrhine species were previously reported in Taylor and Vinyard (2004, 2009) while the strepsirrhine data have never been previously published. All but two of the platyrrhine and five of the

strepsirrhine individuals were captive and all were dentally adult based on third molar eruption. Much of the material was previously formalin-fixed; however, a handful of individual specimens were previously frozen and then were thawed and fixed in 10% buffered formalin. All samples were stored in 10% buffered formalin until use.

For comparison of our fibre length estimates based on in situ muscle sectioning with data collected using chemical digestion, we gathered published fibre length data from chemically digested muscles of the same 14 strepsirrhine species ($n = 20$ individuals) from Perry et al. (2011; Table 1). Perry et al. (2011) published fibre length estimates for the superficial masseter and for the superficial and deep temporalis; we averaged their reported superficial and deep temporalis fibre lengths for these comparisons. Hartstone-Rose et al. provided us with their unpublished fibre length estimates for masseter and temporalis for 10 platyrrhine species, four of which overlapped with our own sample ($n = 7$ individuals; Table 1). Perry et al. (2011) reported that the strepsirrhine material was either preserved in 10% formalin, in 70% ethanol or frozen since the time of death. Hartstone-Rose et al. (2018) reported that all specimens were captive-raised adults and were frozen.

To address our second aim of exploring the impact of sampling on fibre architecture scaling patterns across platyrrhines (i.e., fibre length and PCSA), we considered fibre architecture of the masseter and temporalis muscles in a larger sample of 22 platyrrhine species (15 genera, $n = 129$ individuals; note the slight increase in species number from 21 to 22 [with the addition of *Saimiri sciureus*] and the slight increase in number of individuals from Taylor et al., 2015). These data were considered in bootstrapping procedures (see section 2.3) and compared to scaling results for platyrrhines from Hartstone-Rose et al. (2018). Tissue preservation was similar to that described for the first aim.

2.2 | Data collection

Following previously published protocols (e.g., Anapol, 1984; Anapol & Barry, 1996; Anapol et al., 2008; Shahnoor, 2004; Taylor et al., 2015), we dissected the masseter and temporalis muscles free from their bony attachments and separated the deep from the superficial masseter. We sectioned the superficial masseter muscles along their lengths, resulting in a minimum of two, and a maximum of three segments, depending on muscle size, each segment approximately 1.0 cm thick (see Taylor et al., 2015, fig. 1). The temporalis muscles were sectioned along their lengths into anterior, middle and posterior segments. All muscle segments were oriented to view the fibres in cross-section. For each segment of the superficial masseter, anterior and posterior sampling sites were selected along the length of the muscle. For each segment of the temporalis, proximal and distal sampling sites were selected for both the superficial and deep portions of the muscle. For each muscle, up to six adjacent fibres were measured from each sampling site and the average used for analysis. Both Perry et al. (2011) and Hartstone-Rose et al. (2018) report that, because the jaws of their specimens were all at or near occlusion, they did not normalize their fibre lengths to adjust for the effects of differences in jaw posture at time of fixation. Thus, we similarly included only individuals whose jaw postures were at occlusion at the time of fixation and report only on raw fibre lengths (i.e., fibres not normalized to a standard sarcomere length; cf. Anapol & Barry, 1996; Taylor et al., 2015). We weighed each muscle, estimated fibre pinnation, and used the following equation to estimate masseter and temporalis PCSAs (Anapol & Jungers, 1986; Lieber, 2010; Sacks & Roy, 1982):

$$\mathrm{PCSA} = \frac{M * \cos\theta}{L_f * \rho}$$

where M = muscle mass, θ is pinnation angle, L_f is measured fibre length and ρ is muscle density, given as 1.0564 g/cm^3 following Murphy and Beardsley (1974).

2.3 | Data analysis

Hartstone-Rose et al. (2018) did not publish their architecture data (mass, L_f or PCSA) for any of the four jaw adductor muscles (but see Deutsch et al., 2019 for total jaw adductor PCSAs). Hartstone–Rose shared their platyrrhine data for the masseter and temporalis muscles on condition that we not publish the raw data. Thus, to address the hypothesis that L_f estimates from chemical digestion are consistently longer than L_f estimates from in situ sectioned muscles, we mean-centred data for each species to the mean of our sectioned muscle sample for both the Hartstone-Rose et al. (2018) and Perry et al. (2011) datasets. By subtracting the species mean of the in situ sectioned muscle sample from all fibre lengths, we preserve the original units and could readily determine if chemically dissected L_f estimates were larger (i.e., positive values) or smaller (i.e., negative values) than the average L_f obtained from in situ sectioned muscles in each species. We mean-centred the chemically digested Perry et al. (2011) and Hartstone-Rose et al. (2018) data to our dissected averages because our sample sizes were generally larger. Combining the Perry et al. (2011) and Hartstone-Rose et al. (2018) datasets yielded 18 overlapping species with our own data (Table 1). All datasets had L_f estimates for the masseter but not for the

TABLE 2 Mean-centred data for the platyrrhine and strepsirrhine samples. Because data are mean-centred, the estimated mean is zero for all values. In 17 of 32 comparisons (53.13%), fibre length estimates based on chemical dissection (Perry et al., 2011; Hartstone-Rose et al., unpub. data) were longer than estimates based on in situ muscle sectioning. The probability of achieving longer fibres is non-significant (0.43, $p > 0.05$).[a,b]

Species	Superficial masseter		Temporalis	
	This study	Perry et al., 2011	This study	Perry et al., 2011
	Range/estimate	Estimate	Range/estimate	Estimate
Cheirogaleus medius	−0.15 to 0.18	−0.52	−0.13 to 0.13	−0.02
Eulemur coronatus	−0.17 to 0.17	−1.79	0.00	−1.53
Eulemur macaco	0.00	−4.33	-	-
Eulemur mongoz	*−1.61 to 1.07*	**0.46**	-	-
Galago senegalensis	0.00	**0.82**	-	-
Hapalemur griseus	*−2.57 to 3.61*	**0.66**	−1.53 to 2.04	−0.06
Lemur catta	−1.72 to 1.70	−0.90	*−1.50 to 1.20*	**0.40**
Mirza coquereli	0.00	−0.64	0.00	−1.58
Nycticebus coucang	−0.35 to 0.26	**2.74**	−0.50 to 0.87	**2.38**
Nycticebus pygmaeus	0.00	−0.19	-	-
Otolemur garnetti	−0.80 to 0.58	**0.79**	0.00	−1.24
Propithecus coquereli	−1.08 to 0.55	**2.92**	−1.32 to 1.32	−1.10
Propithecus tattersalli	−0.44 to 0.44	**3.81**	−1.63 to 1.63	**3.69**
Varecia rubra	*−0.71 to 0.38*	**0.73**	0.00	**0.66**
	Masseter		**Temporalis**	
	This study	Hartstone-Rose et al. (unpub. data)	This study	Hartstone-Rose et al. (unpub. data)
	Range	Estimate	Range	Estimate
Callithrix jacchus	*−1.30 to 1.26*	**0.96**	−2.43 to 2.24	**2.49**
Saguinus oedipus	*−0.85 to 1.33*	**1.02**	−0.81 to 0.64	**3.64**
Saimiri sciureus	*−4.04 to 5.47*	−1.21	*−2.46 to 2.52*	**1.71**
Sapajus apella	*−2.48 to 7.29*	−1.65	*−5.46 to 9.84*	−5.05

[a]Bolded values indicate L_f estimates from Perry et al. (2011) and Hartstone-Rose et al. (unpub. data) that exceed our estimates. See Table S1 for raw data (means/single specimen values and ranges) for the strepsirrhine samples included in this study.

[b]Italicized ranges indicate that the greater L_f estimates from Perry et al. (2011) and Hartstone-Rose et al. (unpub. data) fell within our range for that species, their shorter L_f estimate fell within our range, or our estimate fell within their range (*V. rubra*; see Table S1). Thus, for a total of 22/32 comparisons (69%), our fibre length estimates were either longer than or our ranges overlapped with those of Perry et al. (2011) (and Hartstone-Rose et al. (2018).

temporalis. Based on overlapping species and muscles, this yielded 18 comparisons for the masseter and 14 for the temporalis for a total of 32 comparisons (Table 2). For the strepsirrhine sample, we provide our raw L_f estimates for all our in situ sectioned masseter and temporalis muscles alongside those published by Perry et al. (2011) (Table S1).

As a retrospective study, rather than one directly comparing chemical digestion and dissection methods in the same muscle from the same individual, we consider an individual's L_f for a given muscle in a given species to be represented by the sum of multiple components:

$$L_f = L_{f-ave} + L_{f-ind} + L_{f-m-method} + L_{f-m-oth} + L_{f-error}$$

where L_f is the sum of the species average fibre length ($L_{f\text{-}ave}$) plus an individual effect ($L_{f\text{-}ind}$), an effect of measurement method ($L_{f\text{-}m\text{-}method}$), other aspects of the measurement process not considered here ($L_{f\text{-}m\text{-}oth}$) and measurement error as well as preservation effects on individual specimens ($L_{f\text{-}error}$). Based on this model, we used a binomial test (GraphPad Prism v. 9.0.2, GraphPad Software) to assess the hypothesis that chemical dissection results in significantly longer fibres. In this test, chemically dissected fibres should be consistently longer than the average L_f obtained from in situ muscle sectioning

(i.e., positive values relative to the in situ muscle sectioning mean = 0) significantly more frequently than by chance (i.e., 50/50) if measurement method ($L_{f\text{-}m\text{-}method}$) has a significant impact on L_f. A non-significant result indicates that the chemical dissection method does not meet the threshold for exceeding other variables that contribute to L_f variation in a species. We classified every chemical fibre length estimate that was longer than the in situ muscle sectioned estimate as a 'success' (x) and the total number of species comparisons for each group as the trials (n). We set the probability at 0.5 (i.e., a 50/50 chance that the chemical digestion method yields longer fibres for any individual species). We considered this probability to provide a test in favour of the hypothesis since a hypothesis of consistently longer fibres would suggest a positively skewed distribution (i.e., a greater than 50/50 chance of longer fibres). We considered the cumulative probability of achieving longer fibres to be significant at $p < 0.05$.

To address our second aim of exploring the effect of sampling on scaling patterns of architectural measures across platyrrhines, we applied a bootstrapping approach to assess the impact of key differences in sampling between Hartstone-Rose et al. (2018) and Taylor et al. (2015). In all scaling comparisons, we created bootstrapped samples for each species mean for superficial masseter L_f and $PSCA^{0.5}$ as well as jaw length using our dataset. For each species, we created 10,000 replicate means for each of these three variables based on a normal distribution applying the measured mean, standard deviation and sample size available for that specific species to the resampling parameters. In cases where a species was represented by a single individual, that value was applied to all slope calculations. Each bootstrapped distribution yielded an RMA slope estimate, and associated p-value for significance of the slope estimate and correlation coefficient between the architectural variable and jaw length. We compared the distributions of these 10,000 interspecific slopes, p-values and correlation coefficients between sampling approaches used in the two studies.

We compared three different sampling approaches. Initially, we created bootstrapped scaling metrics from our platyrrhine sample (Taylor et al., 2015) to match the 10 species included in Hartstone-Rose et al. (2018). To do this, we used as many overlapping genera and species as possible, approximating the size range of their 10 platyrrhine species used in Hartstone-Rose et al. (2018) and using the same number of individuals as in their samples. We call this the 'small sample, few species' model (SS-FS). We then re-sampled from our platyrrhine sample using the same 10 species as in our SS-FS model while including our larger intraspecific sample sizes in each species' bootstrap of mean values. We call this the 'large sample, few species' model (LS-FS). For the means and standard deviations, we used our data because the majority of the platyrrhine data in Hartstone-Rose et al. (2018) were samples of $n = 1$ without standard deviations. Finally, we created scaling measurements using both the larger numbers of species and larger number of individuals per species—'large sample, many species' model (LS-MS). In addition to graphical and descriptive comparisons of distributions, we used a nonparametric Kolmogorov–Smirnov Two-Sample test (K–S test) to determine differences among resulting distributions. All resampling and statistical comparisons were completed in Systat 13 (Systat Software, Inc.). All figures were created in OriginPro 2023 (OriginLab Corporation). The species and sample sizes employed by Hartstone-Rose et al. (2018) and in each of our three models using our platyrrhine data are given in Table S2.

3 | RESULTS

3.1 | Comparison of fibre lengths

For the combined strepsirrhine and platyrrhine samples ($n = 18$ overlapping species), L_f estimates comprising both mean values and values for single individuals as reported by Perry et al. (2011) and Hartstone-Rose et al. (unpublished data) were longer than our estimates for 17/32 comparisons (53.13%; Table 2). Chemical digestion resulted in longer L_f estimates for 10 masseter and seven temporalis muscle comparisons (Table 2). Treating an estimate of longer fibres based on chemical digestion as a 'success', the probability of achieving longer fibres for at least 17/32 comparisons is 0.43, which is >0.05 and thus not statistically significant.

3.2 | Impact of sampling on platyrrhine muscle scaling

Bootstrapped distributions of platyrrhine species means suggest two basic shifts in RMA slope estimates for superficial masseter L_f and PCSA as intraspecific samples increase (SS-FS vs. LS-FS) and as interspecific samples are added (LS-MS vs. SS-FS and LS-FS) (Table 3; Figures 1a and 2a). The increase in intraspecific sample sizes does not markedly change the average slope estimate for the 10 platyrrhine species sampled, but drastically reduces the range of slopes in the distribution almost 7× when going from SS-FS to LS-FS (Table 3; Figures 1a and 2a). In this case, increased intraspecific sampling markedly decreases the dispersion of slope estimates. Alternatively, the increase to 22 species in the

TABLE 3 Summary statistics (i.e., mean, variance, CV and range) of 10,000 bootstrapped results for reduced major axis (RMA) slopes, correlations, and *p*-values for the 'Small sample, few species' (SS-FS), 'Large sample, few species' (LS-FS) and 'Large sample, many species' (LS-MS) models.

	Superficial masseter fibre length (L_f, mm)			**Superficial masseter PCSA$^{0.5}$**		
	SS-FS	**LS-FS**	**LS-MS**	**SS-FS**	**LS-FS**	**LS-MS**
	RMA slope	RMA slope	RMA slope	RMA slope	RMA slope	RMA slope
Mean	1.27	1.10	0.86	1.64	1.50	0.99
Variance	0.11	0.02	0.004	0.29	0.11	0.01
CV	0.26	0.11	0.08	0.33	0.23	0.11
Min–Max (range)	0.54–7.43 (6.89)	0.71–1.65 (0.94)	0.65–1.95 (1.31)	0.43–7.11 (6.68)	0.83–7.06 (6.24)	0.81–2.99 (2.18)
	Correlation L_f-JL	**Correlation L_f-JL**	**Correlation L_f-JL**	**Correlation PCSA-JL**	**Correlation PCSA-JL**	**Correlation PCSA-JL**
Mean	0.47	0.56	0.79	0.53	0.59	0.78
Variance	0.02	0.006	0.003	0.07	0.04	0.005
CV	0.33	0.14	0.07	0.49	0.36	0.09
Min–Max (range)	−0.34–0.86 (1.20)	0.24–0.79 (0.55)	0.27–0.92 (0.65)	−0.79–0.97 (1.76)	−0.43–0.88 (1.31)	0.18–0.89 (0.70)
	***p*-value**	***p*-value**	***p*-value**	***p*-value**	***p*-value**	***p*-value**
Mean	0.21	0.11	<0.001	0.18	0.13	0.001
Variance	0.03	0.004	<0.001	0.06	0.04	<0.001
CV	0.85	0.58	15.7	1.34	1.62	10.18
Min–Max (range)	0.001–0.999 (0.998)	0.006–0.51 (0.50)	<0.001–0.23 (0.23)	<0.001–0.999 (0.999)	0.001–0.998 (0.997)	<0.001–0.41 (0.41)

Abbreviation: JL, jaw length.

LS-MS model further reduces variance (but not range), while markedly shifting the average slope estimates compared to the two distributions with fewer species (Figures 1a and 2a). The shift in average slope estimates likely reflects two factors. First, the 22 species span a larger range of platyrrhine sizes (see Section 4). Second, size-correlated biological differences in architectural variables between the species in the larger sample (LS-MS) versus the restricted species sampling likely impact the shift in slope estimates. In this case, failure to broadly sample the clade in the 10 species samples likely provides slope estimates that do not accurately represent platyrrhines as a group.

Given the visual differences in slope distributions among the three sampling approaches (Figures 1a and 2a), it is not surprising that all pairwise comparisons of slope estimate distributions using the K–S two-sample tests are significantly different ($p < 0.001$) (Table 4). Also not surprisingly, the greatest Kolmogorov D (Distance) statistics are found between the LS-MS versus the two 'Few Species' distributions, further emphasizing the significance of species sampling when looking at allometric patterns across a clade.

The distributions of correlations between architectural measurements and jaw length as well as the distributions of *p*-values for slope estimates also change consistently across the three sampling regimes. As might be expected, correlation estimates increase and dispersion of correlation estimates decreases as more specimens are sampled from SS-FS to LS-FS and ultimately LS-MS (Table 3; Figures 1b,c and 2b,c). Alternatively, *p*-value estimates decrease as sampling improves across the three distributions. The LS-MS sample demonstrates a marked reduction in variance of *p*-values supporting the statistical importance of broadly sampling a clade.

4 | DISCUSSION

4.1 | Impact of methodological approach versus sampling on fibre length estimates

In this study, we tested the hypothesis that chemical digestion results in systematically longer estimates of L_f when compared with L_f measured in situ using sectioned muscle bellies. Based on our strepsirrhine and platyrrhine comparisons, we found no evidence to support this hypothesis: the probability of obtaining a

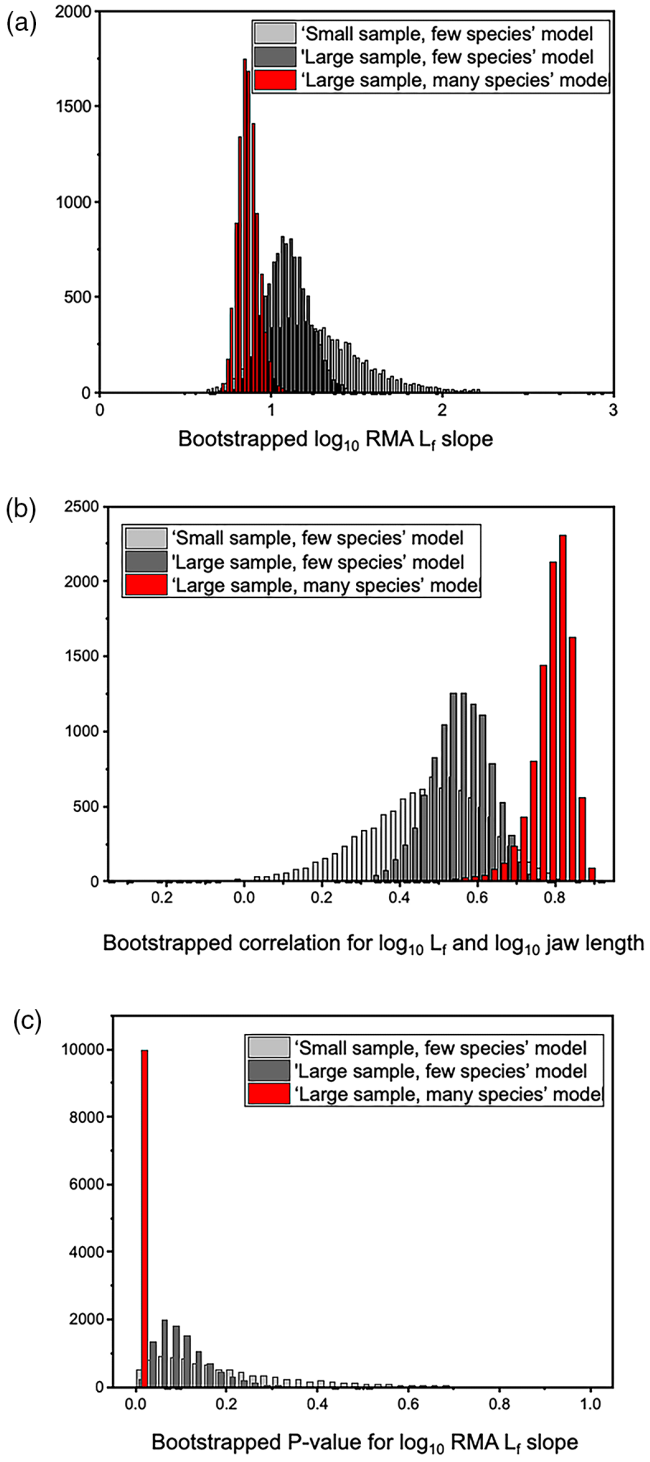

FIGURE 1 Bootstrapped distributions of platyrrhine species. (a) RMA slope estimates for Log_{10} superficial masseter fibre length (L_f) regressed on Log_{10} jaw length, (b) correlations for Log_{10} L_f and Log_{10} jaw length and (c) *p*-values for RMA slope estimates. Small sample-few species (SS-FS) are shown in light gray, Large sample-few species (LS-FS) in dark gray and Large sample-many species (LS-MS) in red. Note the reduced dispersion as sample sizes increase and the major shift in average slope estimates in the 'many species' compared to 'few species' models.

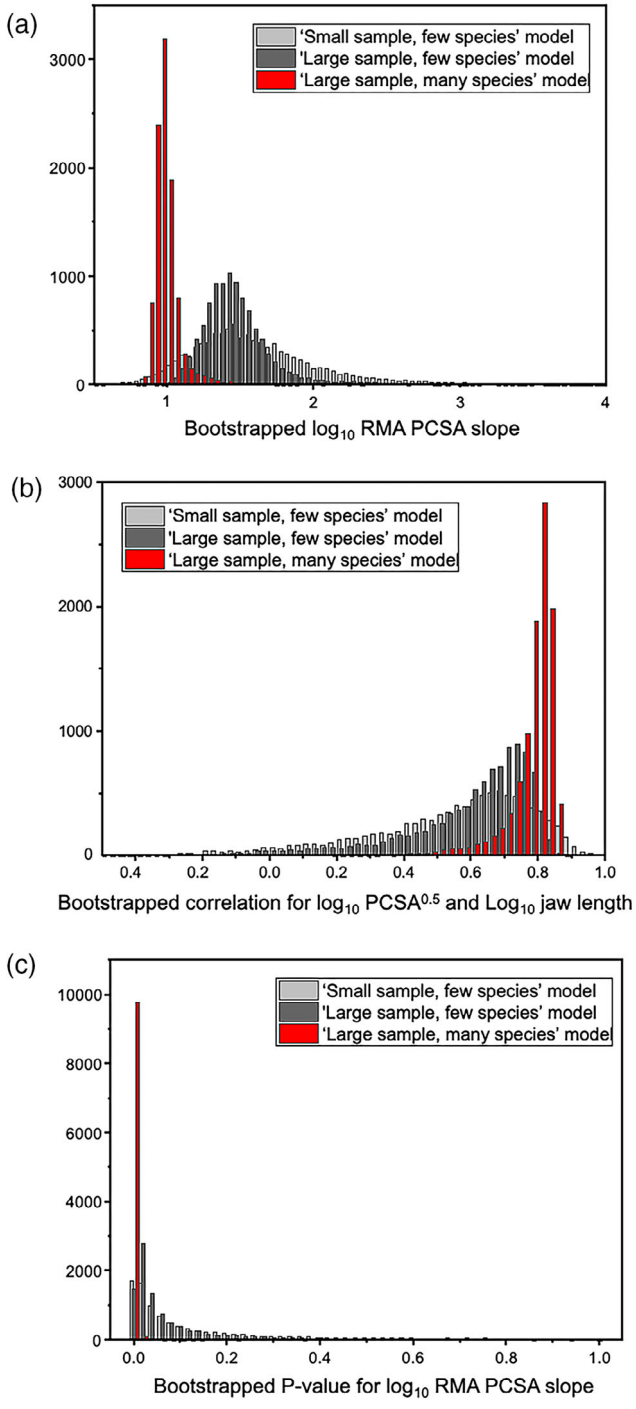

FIGURE 2 Bootstrapped distributions of platyrrhine species. (a) RMA slope estimates for Log_{10} superficial masseter $PCSA^{0.5}$ regressed on Log_{10} jaw length, (b) correlations for Log_{10} $PCSA^{0.5}$ and Log_{10} jaw length and (c) *p*-values for RMA slope estimates. Small sample-few species (SS-FS) are shown in light gray, Large sample-few species (LS-FS) in dark gray and Large sample-many species (LS-MS) in red. Note the reduced dispersion as sample sizes increase and the major shift in average slope estimates in the 'many species' compared to 'few species' models.

TABLE 4 Results of the Kolmogorov–Smirnov two-sample tests of pairwise comparisons of slope estimates and maximum distances between models.

Superficial masseter fibre length	SS-FS	LS-FS	LS-MS
SS-FS		0.362	0.815
LS-FS	<0.0001		0.818
LS-MS	<0.0001	<0.0001	
Superficial masseter PCSA			
SS-FS		0.228	0.829
LS-FS	<0.0001		0.914
LS-MS	<0.0001	<0.0001	

Note: *p*-values are below the diagonal, distances are above the diagonal.
Abbreviations: LS-FS, large sample, few species; LS-MS, large sample, many species; SS-FS, small sample, few species.

longer L_f estimate using chemical digestion versus in situ muscle sectioning is no greater than chance.

Insight into the impact of sampling on fibre length estimates can be gleaned by taking a closer look at the data. The strepsirrhine samples used in this study are both relatively small. A number of the species in both the Perry et al. (2011) and our samples are represented by a single individual ($n = 9$ in Perry et al., 2011, $n = 4$ in our dataset) and the maximum species sample size across both datasets is $n = 6$ (*Hapalemur griseus*, Table 1). By contrast, our sample sizes for the four platyrrhine species that overlap with those reported by Hartstone-Rose et al. (2018) are considerably larger ($n = 11$–19 vs. $n = 1$–3, respectively; Table 1). Small samples precluded statistical tests of mean differences between species. However, in the current study, we provide ranges for 16 of 24 muscle comparisons for the strepsirrhine sample; for seven of these, the Perry et al. (2011) L_f estimates fall within our ranges (Table 2; see also Table S1). Where it was possible to qualitatively compare means and ranges (i.e., *H. griseus*, *Propithecus coquereli* and *Varecia rubra*), it is evident that a mean value based on a few individuals does not reliably capture sample variation (Table 2; Table S1). In the case of *H. griseus*, for example, despite a larger mean L_f value for the superficial masseter based on chemical digestion (9.4 [$n = 2$] vs. 8.74 [$n = 6$] based on in situ sectioning), our mean estimate falls well within the species range reported in Perry (2008), the Perry (2008) mean estimate falls well within our range, and our sample of six extends both ends of the species range beyond that reported by Perry (2008) (Table 2; Table S1). Likewise, our mean superficial masseter L_f of 11.67 for *V. rubra* falls comfortably within the range reported by Perry (2008) even though our mean value is smaller. With our larger platyrrhine sample sizes, six of eight (75.0%) L_f estimates reported by Hartstone-Rose (unpub. data) fall within our ranges, even if their L_f estimate (based on either a single individual or a mean) exceeded ours (Table 2). This within-species variation is likely more influential on L_f estimates than methodological approach (compare the bootstrapped slopes, correlations and *p*-values between the 'Small sample, few species' and 'Large-sample, few species' models; Figure 1).

Across a range of human and nonhuman primate muscles, previous studies that report standard deviations, coefficients of variation and/or ranges for estimates of L_f for a given muscle show a fair amount of variation within a single adult individual (e.g., Charles et al., 2022; Dickinson et al., 2018; Perry, 2008), between sexes of a given species (e.g., Terhune et al., 2015) and within species (e.g., Anapol & Jungers, 1986; Antón, 1999; Butcher et al., 2019 Supplementary Information; Huq et al., 2015; Mathewson et al., 2014; Oishi et al., 2008; Organ et al., 2009; Perry, 2008; Taylor & Vinyard, 2013; Taylor et al., 2015; van Eijden et al., 1997; Ward et al., 2009). For their digital reconstructions of superficial masseter, deep masseter and temporalis on a single specimen of *C. jacchus*, Dickinson et al. (2018) report standard deviations (SD) that were sufficiently large to comfortably accommodate their reported L_f estimates based on in situ measurements from sectioned muscle bellies from the same individual; the reported within-muscle variation (based on the SDs of the digitally-reconstructed fibres) was actually greater than the differences in L_f estimates between the methods.

We acknowledge that in the current study there will be some variation related to the fact that the L_f estimates derived from chemical digestion and those measured in situ from sectioned muscle bellies were obtained from different individuals. The ideal comparison would use measurements taken from right and left sides of the same individuals. Nevertheless, that component of interindividual variation has not masked the components of variation directly considered in this analysis—the effects of species average ($L_{f\text{-ave}}$), individual ($L_{f\text{-ind}}$) and measurement method ($L_{f\text{-m-method}}$). Based on our results and considering the variation reported in other studies, we conclude that

within-species and within-individual sample variation is high, and more than sufficient to account for the observed differences between our L_f estimates and those of Perry et al. (2011) and Hartstone-Rose et al. (unpub. data), irrespective of methodological differences.

4.2 | The impact of sampling on scaling of fibre length and PCSA in platyrrhines

Sampling also accounts for observed differences in scaling between Hartstone-Rose et al. (2018) and Taylor et al. (2015). In their scaling analysis of platyrrhine jaw-closing muscles, Hartstone-Rose et al. (2018) sampled 10 species (7 genera, 14 individuals) ranging in body size from *Callithrix jacchus* (317 g) to *Chiropotes sagulatus* (3000 g) (body mass data reported in Hartstone-Rose et al., 2018, taken from Fleagle, 2013). In Taylor et al. (2015), we evaluated the scaling relationships of the superficial masseter and temporalis muscles in 21 species (15 genera, 116 individuals) that ranged in body size (as reported in Smith & Jungers, 1997) from *Cebuella pygmaea* (110 g for males) to *Lagothrix lagotricha* (7280g to >9270 g for males), thereby capturing nearly the full range of body size across the entire clade.[1] We also included species with body sizes on the higher end of the size distribution for platyrrhines, including *Ateles geoffroyi*, *Alouatta seniculus* and *Alouatta palliata*, taxa that were not included in Hartstone-Rose et al. (2018). Our sample captured the range of body sizes included in Hartstone-Rose et al. (2018) as well as body sizes 100%–200% larger than their largest species. Considered another way, their body size range of 317–3000 g represents a 10-fold difference between the smallest and largest species; our body size range of 110–9270 g represents an 84-fold difference.

Our bootstrapped results, in which we used as many overlapping species and genera as possible and approximated the size range of the 10 platyrrhine species included in Hartstone-Rose et al. (2018), demonstrate overlap in L_f and PCSA slopes between our 'small sample, few species' (SS-FS) and 'large sample, few species' (LS-FS) models. In this comparison the LS-FS model shows a subtle shift and narrowing of the sample distributions for the slopes, correlations and *p*-values (Figures 1a,b and 2a,b). As these two models comprise the same taxa and differ only in number of data points within species (i.e., 14 data points in the SS-FS model to simulate the sample size in Hartstone-Rose et al., 2018 and 82 data points in the LS-FS model to generate the species means for the same set of taxa used in the SS-FS model), these results speak to the influence of intraspecific sample sizes on the variation in regression slopes for these two architectural parameters. However, where we observe the greatest shifts in sample distributions is between these two models and the 'Large sample, many species' (LS-MS) model, which included 12 additional species and sampled from nearly the full body size range across the clade. (Figures 1 and 2). These results speak to the influence of both species number and size range on the scaling relationships for L_f and PCSA. Whereas the LS-FS model increases the reliability because we more accurately estimated each species mean in the model, the LS-MS model increases the validity within the clade because we sampled more thoroughly throughout the clade space rather than extrapolating from a sample of 10 species.

4.3 | Platyrrhine jaw-muscle allometry redux

In our 2015 paper, Taylor and colleagues found that L_f and PCSA of the superficial masseter and temporalis muscles scale with significant negative allometry, such that as platyrrhines increase in size, the excursion and force-generating abilities of these two muscles decrease in comparison with smaller-bodied species. Using phylogenetic generalized least-squares regression (PGLS), we reported phylogenetic correlations between estimates of L_f and jaw length, condyle-M_1 length and body mass of 0.785, 0.787 and 0.742 for the superficial masseter and 0.908, 0.885 and 0.858 for the temporalis, respectively. Hartstone-Rose et al. reported correlations between their L_f estimates and jaw length, a cranial geometric mean and body mass of 0.61, 0.70 and 0.64 for the masseter and 0.14, 0.24 and 0.16 for the temporalis, noting that for all but masseter L_f versus their cranial geometric mean, the correlations were 'too insignificant for attribution of confidence intervals' (2018, p. 321). Despite these low correlations, they reported reduced-major axis (RMA) regression coefficients and concluded that 'For most muscles and groups, there appears to be a tendency toward negative allometry of [fibre length]' (Hartstone-Rose et al., 2018, p. 318). In other words, both studies converged on the conclusion that fibre lengths for these muscles scale with negative allometry in platyrrhines. However, with much higher correlations than those associated with L_f, Hartstone-Rose et al. (2018) also reported that masseter PCSA scales with strong positive allometry relative to body mass and jaw length. For temporalis PCSA, they reported positive allometry and isometry relative to body mass and jaw length, respectively.

These two disparate results for PCSAs are reconciled by consideration of the specific taxa included in the two sets of analyses, and we believe this addresses the question of how to account for these differences in scaling between these two studies. As is apparent from our

TABLE 5 Reduced major axis (RMA) regression slopes, correlations (r), sample sizes (n), degrees of freedom (df) and 95% CIs about the slopes for superficial masseter $PCSA^{0.5}$ versus jaw length for the 'Small sample, few species' (SS-FS) and 'Larges sample, many species' (LS-MS) models compared with results reported by Hartstone-Rose et al. (2018).

Superficial masseter $PCSA^{0.5}$ versus jaw length	RMA slope	r	n	df	95% CI
SS-FS model (species means)[a]	1.32	0.66	10	1,8	0.52–2.13
LS-MS model (species means)[b]	0.94	0.83	22	1,20	0.69–1.19
Hartstone-Rose et al. (2018)[c]	1.62	0.94	—[d]	—[d]	1.17–2.23

[a]The data in this RMA regression include nine species from Taylor et al. (2015) plus *Saimiri sciureus* ($n = 10$ platyrrhine species means; see Table S2).
[b]The data in this RMA regression include the original 21 platyrrhine species from Taylor et al. (2015) plus the addition of *Saimiri sciureus* ($n = 22$ platyrrhine species means; see Table S2).
[c]Hartstone-Rose et al. (2018) do not report the sample sizes used in each of the regression analyses, but we assume the total number of specimens used in this regression is the same as that listed in their Table 1.
[d]Hartstone-Rose et al. (2018) do not report the degrees of freedom or whether they used individual data points or species means in their regression analyses.

bootstrapped distributions for the SS-FS and LS-FS models (Figure 2a,b), had we restricted our scaling analysis of PCSA to the same or similar taxa as those included in Hartstone-Rose et al. (2018), these two studies would have yielded comparable scaling results, that is, positive allometry of PCSA relative to jaw length. To demonstrate this another way, following Hartstone-Rose et al. (2018), we ran a RMA regression of superficial masseter PCSA versus jaw length using our SS-FS and LS-MS datasets. In the first case, the RMA slope was positive (Table 5), consistent with those reported for Hartstone-Rose et al. (2018). However, the slope using the LS-MS dataset was negatively allometric—consistent with results reported by Taylor et al. (2015). We interpret these findings to indicate that inclusion in our sample of larger-bodied taxa not included in Hartstone-Rose et al. (2018), such as *Ateles*, *Alouatta* and *Lagothrix*, is an important driver of these differences in regression slopes. We can further note that in a similar analysis by Anapol et al. (2008) using body mass as the independent variable, their RMA slope for the masseter of 1.19 fell within the 95% CIs for negative and positive allometry as well as isometry (95% CI = 0.39), but their slope was clearly less than the slope of 1.95 reported by Hartstone-Rose et al. (2018).

Harkening back to Fleagle (1985, p. 8), it may be instructive to consider scaling of the chewing muscles in platyrrhines within the relevant ecological framework of feeding behaviour and diet and ask the question, 'What can (or must) large primates do better than small ones, and vice versa?' As discussed in Taylor et al. (2015), among the relatively smaller-bodied taxa in our sample are a number of seed predators such as *Chiropotes*, *Sapajus apella*, *Pithecia*, *Callicebus* and *Cacajao*, while the larger-bodied taxa—atelids and howlers—feed predominantly on ripe fruits and leaves of relatively low toughness, respectively (Cant, 1990; Di Fiore et al., 2011; González-Zamora et al., 2008; Milton, 1978; Teaford et al., 2006). A size-correlated decrease in masseter and temporalis PCSAs would signal that the smaller-bodied taxa, which feed on some mechanically challenging food items, are capable of generating relatively larger maximal muscle and bite forces compared to the larger-bodied taxa, which feed on some of the least mechanically challenging foods. At the same time, the larger-bodied taxa benefit simply by being larger and thus able to generate absolutely larger maximal muscle and bite forces compared to the smaller ones. The clade-based scaling relationships we observe for the superficial masseter and temporalis are consistent with this ecological context. Whether the appropriate independent variable is body mass, jaw length or some other variable (e.g., craniobasal length; Anapol et al., 2008), and whether PGLS, RMA or ordinary least-squares regression slopes are closer to the true nature of these scaling relationships can all be debated. Likewise, biomechanical and evolutionary arguments can be made in favour of negative as well as positive allometry (e.g., Anapol et al., 2008) of the jaw adductors in platyrrhines as well as other primates. Invoking differences in methods of data collection to explain differences across studies in scaling relationships of the jaw adductors in platyrrhines obfuscates that these differences are easily reconciled by differences in sampling strategy and statistical approach.

4.4 | Epilogue

Here we have shown that the probability of obtaining longer fibres based on muscles chemically digested versus muscles sectioned along their bellies is no greater than chance. We thus find little evidence to support the hypothesis that use of one or the other methodological approach has a consequential impact on estimates of L_f or PCSA. When considering the amount of intraindividual and intraspecies variation in L_f and PCSA reported across studies, we suggest this variation is likely to be far more important in accounting for differences in L_f

between our two studies than differences in our methodological approaches. Alternatively, sampling differences between our two studies can account for differences in scaling results: we essentially replicate the positive scaling of PCSAs reported by Hartstone-Rose et al. (2018) when using a dataset similar in species composition (compare SS-FS with LS-FS; Figure 2a,b) while at the same time support our original conclusion that platyrrhine superficial masseter and temporalis PCSAs scale with negative allometry when evaluated in a sample effectively representing a clade in terms of body size and behavioural ecology (Figure 2c; Tables 3 and 5).

An additional consideration in achieving a reliable estimate of L_f within individuals and species is the number of sampled fibres within a given muscle. A thousand random subsamples from 5000 measured fibres obtained on 25 different lower limb muscles for a sample of 10 humans shows large intraindividual and intraspecies errors in L_f and PCSA for samples of <250 fibres (Charles et al., 2022). While statistically this is probably not surprising, it highlights one aspect of variation that has been almost universally overlooked and underappreciated in studies of fibre architecture; essentially all of the architectural studies we cite in this paper with the exception of Dickinson et al. (2018), including our own, are likely undersampling the number of fibres per muscle. Inadequate sampling of fibre number may result in elevated levels of random variation with the potential to obscure interpretations of muscle function within and between species (Charles et al., 2022).

In sum, while we agree that different methods of collecting architecture data have the potential to produce different results between or among studies, variation due to sampling would seem to far surpass variation due to such methodological differences when comparing between Taylor et al. (2015) and Hartstone-Rose et al. (2018). Larger sample sizes within species to adequately capture species means, larger numbers of species that span the full range of body size and other relevant ecological variables within a clade, and perhaps larger numbers of measured fibres within muscles, would seem to be more important considerations than muscle methodology for future studies of mammalian muscle architecture and scaling.

AUTHOR CONTRIBUTIONS

Andrea B. Taylor: Conceptualization; investigation; writing – original draft; methodology; validation; visualization; writing – review and editing; formal analysis; project administration; data curation; supervision; resources; funding acquisition; software. **Claire E. Terhune:** Conceptualization; writing – review and editing. **Callum F. Ross:** Conceptualization; writing – review and editing; funding acquisition. **Christopher J. Vinyard:** Conceptualization; investigation; funding acquisition; methodology; validation; visualization; writing – review and editing; writing – original draft; formal analysis; project administration; data curation; supervision; resources; software.

ACKNOWLEDGMENTS

Strepsirrhine material collected by the authors was provided courtesy of the Cleveland Museum of Natural History (CMNH; Cleveland, OH), Museum of Comparative of Zoology (Cambridge, MA), Duke Lemur Center (DLC; Durham, NC), Parc Botanique et Zoologique de Tsimbazaza (Madagascar) and Smithsonian National Museum of Natural History (Washington, DC). Platyrrhine material to collected by the authors was provided courtesy of the Museum of Anthropology (University of Zurich), New England Primate Regional Primate Research Center, Squirrel Monkey Breeding and Research Resource, Smithsonian National Museum of Natural History, the University of Chicago, and Wisconsin Regional Primate Research Center. We are grateful to the Editor and two anonymous reviewers for their comments which helped improve the manuscript.

FUNDING INFORMATION

This study was made possible by grants for the National Science Foundation (BCS 0452160 and 0962677).

DATA AVAILABILITY STATEMENT

The data that support the findings of this study are available in the text and in the Supporting Information of this article.

ORCID

Andrea B. Taylor https://orcid.org/0000-0001-6647-5488
Claire E. Terhune https://orcid.org/0000-0002-5381-2497
Callum F. Ross https://orcid.org/0000-0001-7764-761X
Christopher J. Vinyard https://orcid.org/0000-0002-7355-5192

ENDNOTE

[1] *Alouatta pigra*, at 11,400 g, is the only other platyrrhine with a reported body mass higher than that of *Lagothrix lagotricha* (Smith & Jungers, 1997).

REFERENCES

Abdala, V., Manzano, A. S., & Herrel, A. (2008). The distal forelimb musculature in aquatic and terrestrial turtles: Phylogeny or environmental constraints? *Journal of Anatomy*, *213*, 159–172.

Allen, H. (1880). On the temporal and masseter muscles of mammals. *Proceedings of the Academy of Natural Sciences of Philadelphia*, *32*, 385–396.

Anapol, F., & Jungers, W. L. (1986). Architectural and histochemical diversity within the quadriceps femoris of the Brown lemur (*Lemur fulvus*). *American Journal of Physical Anthropology*, *69*, 355–375.

Anapol, F., Shahnoor, N., & Ross, C. F. (2008). Scaling of reduced physiologic cross-sectional area in primate muscles of mastication. In C. J. Vinyard, M. J. Ravosa, & C. E. Wall (Eds.), *Primate craniofacial function and biology* (pp. 201–215). Springer.

Anapol, F. C. (1984). *Morphological and functional diversity within the quadriceps femoris in Lemur fulvus: Architectural, histochemical, and electromyographic considerations*. PhD Dissertation, State University of New York at Stony Brook.

Anapol, F. C., & Barry, K. (1996). Fiber architecture of the extensors of the hindlimb in semiterrestrial and arboreal guenons. *American Journal of Physical Anthropology*, *99*, 429–447.

Antón, S. C. (1999). Macaque masseter muscle: Internal architecture, fiber length and cross-sectional area. *International Journal of Primatology*, *20*, 441–462.

Bardeen, C. R. (1906). Development and variation of the nerves and the musculature of the inferior extremity and of the neighboring regions of the trunk in man. *American Journal of Anatomy*, *6*, 259–390.

Bijvoet, W. F. (1908). Morphologie des Musculus digastricus mandibulae bei den Säugetieren. *Zeitschrift für Morphologie und Anthropologie*, *11*, 249–316.

Bodine, S. C., Roy, R. R., Meadows, D. A., Zernicke, R. F., Sacks, R. D., Fournier, M., & Edgerton, V. R. (1982). Architectural, histochemical, and contractile characteristics of a unique biarticular muscle: The cat semitendinosus. *Journal of Neurophysiology*, *48*, 192–201.

Butcher, M. T., Rose, J. A., Glenn, Z. D., Tatomirovich, N. M., Russo, G. A., Foster, A. D., Smith, G. A., & Young, J. W. (2019). Ontogenetic allometry and architectural properties of the paravertebral and hindlimb musculature in Eastern cottontail rabbits (*Sylvilagus floridanus*): Functional implications for developmental changes in locomotor performance. *Journal of Anatomy*, *235*, 106–123.

Cant, J. G. H. (1990). Feeding ecology of spider monkeys (*Ateles geoffroyi*) at Tika, Guatemala. *Human Evolution*, *5*, 269–281.

Charles, J., Kissane, R., Hoehfurtner, T., & Bates, K. T. (2022). From fibre to function: Are we accurately representing muscle architecture and performance? *Biological Reviews*, *97*, 1640–1676.

Close, R. I. (1972). Dynamic properties of mammalian skeletal muscles. *Physiological Reviews*, *52*, 129–197.

Curtis, A. A., & Santana, S. E. (2018). Jaw-dropping: Functional variation in the digastric muscle in bats. *The Anatomical Record*, *301*(2), 279–290.

Deutsch, A. R., Dickinson, E., Leonard, K. C., Pastor, F., Muchlinski, M. N., & Hartstone-Rose, A. (2019). Scaling of anatomically derived maximal bite force in primates. *The Anatomical Record*, *303*(7), 2026–2035.

Di Fiore, A., Link, A., & Campbell, C. J. (2011). The atelines: Behavioral and socioecological diversity in a New World monkey radiation. In C. J. Campbell, A. Fuentes, K. C. MacKinnon, M. Panger, & S. K. Bearder (Eds.), *Primates in perspective* (pp. 155–188). Oxford University Press.

Dickinson, E., Stark, H., & Kupczik, K. (2018). Non-destructive determination of muscle architectural variables through the use of diceCT. *The Anatomical Record*, *301*(2), 363–377.

Felder, A., Ward, S. R., & Lieber, R. L. (2005). Sarcomere length measurement permits high resolution normalization of fiber length in architectural studies. *Journal of Experimental Biology*, *208*, 3275–3279.

Fleagle, J. G. (1977). Locomotor behavior and muscular anatomy of sympatric Malaysian leaf-monkeys (*Presbytis obscura* and *Presbytis melalophos*). *American Journal of Physical Anthropology*, *46*, 297–307.

Fleagle, J. G. (1985). Size and adaptation in primates. In W. L. Jungers (Ed.), *Size and scaling in primate biology* (pp. 1–19). Springer.

Fleagle, J. G. (2013). *Primate adaptation and evolution* (3rd ed.). Academic Press.

Gans, C. (1982). The functional significance of muscle architecture: A theoretical analysis. *Advances in Anatomy, Embryology and Cell Biology*, *38*, 115–142.

Gans, C., & Bock, W. J. (1965). The functional significance of muscle architecture—A theoretical analysis. *Ergebnisse der Anatomie und Entwicklungsgeschichte*, *38*, 115–142.

González-Zamora, A., Arroyo-Rodríguez, V., Chaves, Ó. M., Sánchez-López, S., Stoner, K. E., & Riba-Hernández, P. (2008). Diet of spider monkeys (Ateles geoffroyi) in Mesoamerica: Current knowledge and future directions. *American Journal of Primatology*, *71*, 8–20.

Gregory, W. K., & Camp, C. L. (1918). *Studies in comparative myology and osteology*. American Museum of Natural History.

Hartstone-Rose, A. H., Deutsch, A. R., Leischner, A. L., & Pastor, F. (2018). Dietary correlates of primate masticatory muscle fiber architecture. *The Anatomical Record*, *301*(2), 311–324.

Haxton, H. A. (1944). Absolute muscle force in the ankle flexors of man. *Journal of Physiology*, *103*, 267–273.

Herrel, A., & O'Reilly, J. C. (2006). Ontogenetic scaling of bite force in lizards and turtles. *Physiological and Biochemical Zoology*, *79*, 31–42.

Howell, A. B. (1926). The saltatorial rodent *Dipodomys*: The function and comparative anatomy of its muscles and osseus systems. *Proceedings of the American Academy of Arts and Sciences*, *67*, 377–536.

Huq, E., Wall, C. E., & Taylor, A. B. (2015). Epaxial muscle fiber architecture favors enhanced excursion and power in the leaper Galago senegalensis. *Journal of Anatomy*, *227*, 425–540.

Huxley, A. F. (1957). Muscle structure and theories of contraction. *Progress in Biophysics and Biophysical Chemistry*, *4*, 225–312.

Jeffery, N. S., Stephenson, R. S., Gallagher, J. A., Jarvis, J. C., & Cox, P. G. (2011). Micro-computed tomography with iodine staining resolves the arrangement of muscle fibres. *Journal of Biomechanics*, *44*, 189–192.

Lieber, R. L. (2010). *Skeletal muscle structure, function, and plasticity*. Wolters Kluwer/Lippincott Williams & Wilkins.

Mathewson, M. A., Kwan, A., Eng, C. M., Lieber, R. L., & Ward, S. R. (2014). Comparison of rotator cuff muscle architecture between humans and other selected vertebrate species. *The Journal of Experimental Biology*, *217*, 261–273.

Metscher, B. D. (2009). MicroCT for comparative morphology: Simple staining methods allow high-contrast 3D imaging of diverse non-mineralized animal tissues. *BMC Physiology*, *9*, 11.

Milton, K. (1978). Behavioral adaptations to leaf-eating by the mantled howler monkey (*Alouatta palliata*). In G. G. Montgomery (Ed.), *The ecology of arboreal folivores* (pp. 353–549). Smithsonian Institution Press.

Murphy, R. A., & Beardsley, A. C. (1974). Mechanical properties of the cat soleus muscle in situ. *American Journal of Physiology*, *227*, 1008–1013.

Myatt, J. P., Crompton, R. H., & Thorpe, S. K. S. (2011). Hindlimb muscle architecture in non-human great apes and a comparison of methods for analysing inter-species variation. *Journal of Anatomy*, *219*, 150–166.

Oishi, M., Ogihara, N., Endo, H., & Asari, M. (2008). Muscle architecture of the upper limb in the orangutan. *Primates*, *49*, 210.

Organ, J. M., Teaford, M. F., & Taylor, A. B. (2009). Functional correlates of fiber architecture of the lateral caudal musculature in prehensile and nonprehensile tails of the Platyrrhini (primates) and Procyonidae (Carnivora). *The Anatomical Record*, *292*(6), 827–841.

Payne, R. C., Crompton, F. H., Isler, K., Savage, R., Vereecke, E. E., Günther, M. M., Thorpe, S. K. S., & D'Août, K. (2006). Morphological analysis of the hindlimb in apes and humans. I. Muscle architecture. *Journal of Anatomy*, *208*, 709–724.

Penrose, F., Cox, P., Kemp, G., & Jeffery, N. (2020). Functional morphology of the jaw adductor muscles in the Canidae. *The Anatomical Record*, *303*(11), 2878–2903.

Perry, J. M. G. (2008). *The anatomy of mastication in extant strepsirrhines and Eocene adapines*. PhD Dissertation, Duke University.

Perry, J. M. G., Hartstone-Rose, A., & Wall, C. E. (2011). The jaw adductors of strepsirrhines in relation to body size, diet, and ingested food size. *The Anatomical Record*, *294*(4), 712–728.

Pfaller, J. B., Gignac, P. M., & Erickson, G. M. (2011). Ontogenetic changes in jaw-muscle architecture facilitate durophagy in the turtle *Stenotherus minor*. *Journal of Experimental Biology*, *214*, 1655–1667.

Powell, P. L., Roy, R. R., Kanim, P., Bello, M. A., & Edgerton, V. R. (1984). Predictability of skeletal muscle tension from architectural determinations in guinea pig hindlimbs. *Journal of Applied Physiology*, *57*, 1715–1721.

Roberts, T. J., & Scales, J. A. (2002). Mechanical power output during running accelerations in wild turkeys. *The Journal of Experimental Biology*, *205*, 1485–1494.

Sacks, R. D., & Roy, R. R. (1982). Architecture of the hind limb muscles of cats: Functional significance. *Journal of Morphology*, *173*, 185–195.

Santana, S. E., Dumont, E. R., & Davis, J. L. (2010). Mechanics of bite force production and its relationship to diet in bats. *Functional Ecology*, *24*, 776–784.

Santana, S. E. (2018). Comparative anatomy of bat jaw musculature via diffusible iodine-based contrast-enhanced computed tomography. *The Anatomical Record*, *301*(2), 267–278.

Scales, J. A., Stinson, C. M., & Deban, S. M. (2016). Extreme performance and functional robustness of movement are linked to muscle architecture: Comparing elastic and nonelastic feeding movements in salamanders. *Journal of Experimental Zoology*, *325*, 360–376.

Shahnoor, N. (2004). *Morphological adaptations to diet in primate masticatory muscles*. PhD Dissertation, University of Wisconsin-Milwaukee.

Smith, R. J., & Jungers, W. L. (1997). Body mass in comparative primatology. *Journal of Human Evolution*, *32*, 523–559.

Stanchak, K. E., & Santana, S. E. (2018). Asessment of the hindlimb membrane musculature of bats: Implications for active control of the calcar. *The Anatomical Record*, *301*(3), 441–448.

Taylor, A., Terhune, C. E., & Vinyard, C. J. (2019). The influence of masseter and temporalis sarcomere length operating ranges as determined by laser diffraction on architectural estimates of muscle force and excursion in macaques (*Macaca fascicularis* and *Macaca mulatta*). *Archives of Oral Biology*, *105*, 35–45.

Taylor, A., Yuan, T., Ross, C. F., & Vinyard, C. J. (2015). Jaw-muscle force and excursion scale with negative allometry in platyrrhine primates. *American Journal of Physical Anthropology*, *158*, 242–256.

Taylor, A. B., & Vinyard, C. J. (2004). Comparative analysis of masseter fiber architecture in gouging (*Callithrix jacchus*) and nongouging (*Saguinus oedipus*) callitrichids. *Journal of Morphology*, *261*, 276–285.

Taylor, A. B., & Vinyard, C. J. (2009). Jaw-muscle fiber architecture in tufted capuchins favors generating relatively large muscle forces without compromising jaw gape. *Journal of Human Evolution*, *57*, 710–720.

Taylor, A. B., & Vinyard, C. J. (2013). The relationships among jaw-muscle fiber architecture, jaw morphology, and feeding behavior in extant apes and modern humans. *American Journal of Physical Anthropology*, *151*, 120–134.

Teaford, M. F., Lucas, P. W., Ungar, P. S., & Glander, K. E. (2006). Mechanical defenses in leaves eaten by costa Rican howling monkeys (*Alouatta palliata*). *American Journal of Physical Anthropology*, *129*, 99–104.

Terhune, C. E., Hylander, W. L., Vinyard, C. J., & Taylor, A. B. (2015). Jaw-muscle architecture and mandibular morphology influence relative maximum jaw gapes in the sexually dimorphic *Macaca fascicularis*. *Journal of Human Evolution*, *82*, 145–158.

Turnbull, W. D. (1970). Mammalian masticatory apparatus. *Fieldiana: Geology*, *18*, 149–356.

van Eijden, T. M. G. J., Korfage, J. A. M., & Brugma, P. (1997). Architecture of the human jaw-closing and jaw-opening muscles. *The Anatomical Record*, *248*(3), 464–474.

Ward, S. R., Eng, C. M., Smallwood, L. H., & Lieber, R. L. (2009). Are current measurements of lower extremity muscle architecture accurate? *Clinical Orthopedics and Related Research*, *467*, 1074–1082.

Williams, P. E., & Goldspink, G. (1971). Longitudinal growth of striated muscle fibres. *Journal of Cell Science*, *9*, 751–767.

Young, J. W., Foster, A. D., Russo, G. A., Smith, G. A., & Butcher, M. T. (2022). Only the good die old? Ontogenetic determinants of locomotor performance in eastern cottontail rabbits (*Sylvilagus floridanus*). *Integrative and Organismal Biology*, *4*, obab037.

SUPPORTING INFORMATION

Additional supporting information can be found online in the Supporting Information section at the end of this article.

How to cite this article: Taylor, A. B., Terhune, C. E., Ross, C. F., & Vinyard, C. J. (2024). The impact of measurement technique and sampling on estimates of skeletal muscle fibre architecture. *The Anatomical Record*, *307*(9), 3071–3084. https://doi.org/10.1002/ar.25415